A Statistical Model of White Matter Fiber Bundles based on Currents

Stanley Durrleman[1,2], Pierre Fillard[3], Xavier Pennec[1], Alain Trouvé[2], and Nicholas Ayache[1]

[1] Asclepios Team-Project, INRIA - Sophia Antipolis-Méditerranée, France
[2] Centre de Mathématiques et Leurs Applications (CMLA), ENS-Cachan, France
[3] Lab. de Neuroimagerie Assistée par Ordinateur - CEA/Neurospin, Saclay, France

Abstract. The purpose of this paper is to measure the variability of a population of white matter fiber bundles without imposing unrealistic geometrical priors. In this respect, modeling fiber bundles as currents seems particularly relevant, as it gives a metric between bundles which relies neither on point nor on fiber correspondences and which is robust to fiber interruption. First, this metric is included in a diffeomorphic registration scheme which consistently aligns sets of fiber bundles. In particular, we show that aligning directly fiber bundles may solve the aperture problem which appears when fiber mappings are constrained by tensors only. Second, the measure of variability of a population of fiber bundles is based on a statistical model which considers every bundle as a random diffeomorphic deformation of a common template plus a random non-diffeomorphic perturbation. Thus, the variability is decomposed into a geometrical part and a "texture" part. Our results on real data show that both parts may contain interesting anatomical features.

1 Introduction

The primary goal of Computational Anatomy is to study the variability of anatomical structures in populations. This analysis can be used to classify populations (e.g. pathologic versus control), or to drive the segmentation of anatomical structures in new images. Variability measures usually rely on correspondences determined by registration. More generally, shape differences can be captured by the geometrical deformation of one structure onto another. These deformations are used to learn how a prototype structure (called also atlas or template) deform within a population. This requires to define a proper registration method and to infer a statistical model on the deformations between an atlas (to be estimated) and each subject in the population.

While such statistical analysis have already been proposed for sulcal lines [1, 2], and subcortical structures [3, 4], much fewer tools are available for white matter fiber bundles obtained in diffusion MRI. These structures are of great importance as they may contribute to map brain connections between functional areas, or to understand effects of neurological pathologies (like Alzheimer's disease) onto the brain white matter. Most recent approaches are based on the

nonlinear registration of fractional anisotropy (FA) maps [5, 6] or tensor images [7, 8]. The deformation resulting from this image registration is then applied to fibers. In these methods, one may question if the fiber bundles are correctly aligned since the bundling information is not visible in FA or tensor images. Fibers which belong to the same bundle connect specific brain regions together and should therefore be preserved during registration. For this reason, we propose here to use directly fiber bundles as constraints to drive the registration.

Recent approaches measuring variability of fiber bundles rely on point or fiber correspondences between bundles [9–11]. However, tractography algorithms were never shown to produce stable and reproducible results. Thus, the comparison of bundles should not rely on individual fibers or points but rather on the global shape of the bundles. Furthermore, tractography might be valid only locally: the true neuronal pathway may correspond to the union of several pieces of fibers and one should not blindly consider sets of connected points produced by tractography as true fibers. The solution of considering a bundle as an unconnected cloud of points is not satisfactory either, since it does not take into account the local orientation of the bundles encoded by the tangents of the fibers. Therefore, an ideal framework for fiber bundles should be robust to *curve connectivity and sampling*, and should take into account the *local orientation* of the bundle. Similarly, a distance between bundles (used as a dissimilarity measure during registration) should rely *neither on point nor on fiber correspondences*. In this paper, we propose to use the framework based on currents, that precisely models curves as a set of unconnected oriented points. This framework is robust to fiber interruption and provides a dissimilarity metric on curve sets that does not assume any kind of correspondences. Conversely, it is sensitive to the local fiber orientation and to the point density: a single fiber will be unlikely to influence registration, which makes currents naturally robust to outliers. Finally, currents are compatible with the diffeomorphic registration method in [12], and therefore can be used for pairwise registration of fiber bundles.

Once a registration framework of fiber bundles modeled as currents is defined, it can be used to define a statistical model of variability. From the perspective of the deformable models, we consider the bundles of different subjects as random diffeomorphic deformations of an unknown template perturbed by non-diffeomorphic variations (called residues in the sequel). Following the work of [4], we jointly estimate this prototype bundle along with its deformations onto each subject's anatomy. In a second time, statistical analysis of bundles is achieved by a principal component analysis (PCA) of the diffeomorphic deformations and the residues to extract their principal modes of variations. The former accounts for the smooth variations of the template within the population: stretching, shrinking, dilation or torsion, while the later accounts for all variations that cannot be captured by regular diffeomorphisms, called *texture* in the sequel: fiber creation or topology changes. This model is not based on strong assumptions and can therefore retrieve a large range of geometrical variations.

The paper is organized as follows. Sec. 2 shows how currents are used to model fiber bundles and how they are interfaced with a diffeomorphic registration

scheme. The statistical model is developed in Sec. 3. In Sec. 4, we evaluate the method on real data. We compare pairwise registrations of 5 fiber bundles with the alignment obtained from FA and tensors images. Finally, we build the atlas from 6 subjects and analyze the variability of the corticobulbar tract.

2 Fiber Bundles Registration based on Currents

2.1 Fiber Bundles Modeled as Currents

Currents are geometrical objects originally introduced in medical image analysis to model curves and surfaces [12]. In this section, we recall the properties which are relevant for our topic and refer the reader to [12, 13, 4] for more details.

In the framework of currents, a set of fibers is characterized by the way it integrates vector fields. Given ω a square integrable $3D$ vector field, a bundle B made of several fibers F_i integrates ω thanks to:

$$B(\omega) = \sum_{F_i \in B} \int_{F_i} \omega(x)^t \tau_i(x) dx, \tag{1}$$

where $\tau_i(x)$ is the oriented tangent vector of the fiber F_i at point x. A fiber bundle may be seen as a set of wires sending information in one direction at a constant rate. Eq. 1 computes the total rate of information that goes through the orthogonal sections (i.e. equipotential surfaces) of ω. To characterize a fiber bundle, we measure how this quantity varies while the equipotentials of ω varies. For this purpose, we define the test space W, in which ω varies, as the set of the convolutions between any square integrable vector fields and a smoothing kernel. This excludes from W the vector fields with too high spatial frequencies. Formally, W is the reproducing kernel Hilbert space (r.k.h.s.) whose kernel K^W is Gaussian: $K^W(x, y) = \exp(-\|x - y\|^2 / \lambda_W^2) I_3$ for any points $(x, y)^4$. The standard deviation, λ_W, is the typical scale at which the vector fields ω varies spatially. In this setting, any set of smooth curves is a continuous linear mapping from W to $\mathbb{R}$. The space of currents W^* is the space containing such objects.

W^* is a vector space. The addition of two pieces of curves is simply the union of them. In Eq. 1, each fiber F_i or each piece of these fibers can be seen as a current individually: the union of them (their addition) is still a current. For instance, Eq. 1 would not change if each F_i were split into a collection of small segments. *It does not depend on the connectivity of the fibers within the bundle.*

Any current in W^* may be decomposed into an *infinite* sum of delta Dirac currents, which play the role of basis vectors. A Dirac current δ_x^τ is defined by: $\delta_x^\tau(\omega) = \tau^t \omega(x)$. It models an oriented point and encodes the direction τ of the fiber bundle at point x. Each segment of the polygonal lines returned by tractography is approximated by a Dirac current δ_x^τ where x is the center of the segment and τ its direction. This approximation converges in the space of

---

[4] K^W is the Green's function of $L^t L$ for some differential operator L. The inner product in W is defined then by $\langle \omega, \omega' \rangle_W = \langle L(\omega), L(\omega) \rangle_{L^2}$. See [14] for more details.

currents as the sampling of the curves becomes finer. In this sense, the modeling is *weakly sensitive to the sampling* of the fibers. As a consequence, a bundle B is approximated by a *finite* sum over all segments within the bundle: $\sum_i \delta_{x_i}^{\tau_i}$.

In addition, the space of currents W^* is provided with a norm and an inner product, which define a distance between two bundles B and B' as: $\|B - B'\|_{W^*} = \sup_{\|\omega\|_W \leq 1} |B(\omega) - B'(\omega)|$. Following our analogy, this measures the rate of information along the wires of B and the wires of B' that goes through the orthogonal sections of the same ω. We look for the regular ω ($\|\omega\|_W \leq 1$) which makes this difference the largest possible, i.e. that captures the more differences between the two structures. This geometric distance compares bundles globally, *without assuming any kind of fiber or point correspondences between them.* The smaller the standard deviation λ_W, the smaller the scale at which ω varies, the finer the geometrical details captured by this distance.

This distance has a closed form. On the Dirac currents, the inner product is given by $\langle \delta_x^\alpha, \delta_y^\beta \rangle_{W^*} = \alpha^t K^W(x,y)\beta$. By linearity, the inner product between two bundles $B = \sum_{i=1}^n \delta_{c_i}^{\tau_i}$ and $B' = \sum_{j=1}^m \delta_{c_j'}^{\tau_j'}$ is given by:

$$\langle B, B' \rangle_{W^*} = \sum_{i=1}^n \sum_{j=1}^m \tau_i^t K^W(c_i, c_j') \tau_j' \tag{2}$$

This inner product (and hence the distance $\|B - B'\|_{W^*}$) does not require any condition on the curves sampling (n may not equal m, for instance). It compares all pairs of tangents (τ_i, τ_j') weighted by a function of their distance $\|c_i - c_j'\|$.

Since the space of currents is a vector space provided with an inner product, we can directly compute the mean and the covariance matrix of a population of fiber bundles. However, this statistical analysis would not be relevant with unregistered fiber bundles. This will be used, instead, to perform PCA on the residuals that remain after registration.

2.2 Spatially Consistent Registration of Fiber Bundles

Our goal is to align two sets of fiber bundles segmented in images of two different subjects. The algorithm introduced in [12] finds precisely a *consistent deformation of the underlying* $3D$ *space* that best matches two sets of labeled currents. The deformations are chosen as $3D$ diffeomorphisms (smooth deformations with smooth inverses), solution at time $t = 1$ of the flow equation: $\frac{\partial \phi_t(x)}{\partial t} = v_t(\phi_t(x))$, with initial condition $\phi_0 = \mathrm{Id}$ (no deformation). The time-varying vector field $(v_t)_{t \in [0,1]}$ is the speed vector field of the deformation, which is supposed to belong to a r.k.h.s. V with Gaussian kernel K^V. The standard deviation of K^V, λ_V, determines the typical scale of the deformation: the greater, the smoother the deformation. The regularity of the final deformation ϕ_1^v is measured by integrating the norm of the speed vector field over time: $d_V^2(\mathrm{Id}, \phi_1^v) = \int_0^1 \|v_t\|_V^2 \, dt$. The registration consists therefore in minimizing:

$$J(v) = \sum_{i=1}^N \left\| \phi_1^v \star B_i - B_j' \right\|_{W^*}^2 + \gamma d_V^2(\mathrm{Id}, \phi_1^v) \tag{3}$$

where γ is the usual trade-off between fidelity to data and regularity. $\phi \star B$ denotes the geometrical transportation of the fiber bundle B by the diffeomorphism ϕ: each point x moves to $\phi(x)$ and each tangent τ is transformed into $d_x\phi(\tau)$, where $d_x\phi$ is the Jacobian matrix of ϕ. This geometrical transportation is conveyed in the space of currents thanks to $(\phi \star B)(\omega) = B((d\phi)^t \omega o \phi)$, which results simply from a change of variable in Eq. 1. On Dirac currents, we have $\phi \star \delta_x^\tau = \delta_{\phi(x)}^{d_x\phi(\tau)}$.

It is proved that the speed vector field minimizing Eq. 3 *is parametrized* by momenta $\alpha_k(t)$ at the points $x_k(t)$ of the moving bundle B: $v_t(x) = \sum_k K^V(x, x_k(t))\alpha_k(t)$ [12, 15]. Once time is discretized, Eq. 3 is therefore minimized via a gradient descent on the parameters: $(\alpha_k(t_p))$. Moreover, the resulting diffeomorphisms are geodesic. Thanks to Euler-Lagrange equations [15], they are entirely determined by their initial momenta $\alpha_k(0)$: *the tangent-space representation* of the diffeomorphism. The metric on this tangent space is given by $\|\alpha(0)\|^2 = \|v_0\|_V^2 = \alpha(0)^t k^V \alpha(0)$ where k^V is the matrix $(K^V(x_i, x_j))_{i,j}$. From now on, we denote ϕ^α the diffeomorphism ϕ_1^v with initial momenta α.

Applying this registration framework directly to fiber bundles, which may have up to 10^5 segments, raises computational issues. The computation of the data fidelity term in Eq. 3 ($\|\phi_1^v \star B - B'\|_{W^*}$) requires to compare every segments of B with every segments of B', as shown in Eq. 2. Hopefully, this complexity is reduced thanks to the approximation scheme of [13].

3   A Statistical Model of Fiber Bundles

In this section, we show how to use the modeling based on currents and the previous registration tool to define a statistical model on fiber bundles. Following [16, 4], we model our observations as deformations of an unknown prototype bundle (also called template or atlas) perturbed by non-diffeomorphic variations (the residues). Formally, we consider the bundles $(B_i)_{i=1\ldots N}$ (the same bundle for N different subjects) as instances of the following process:

$$B_i = \phi_i \star \bar{B} + \varepsilon_i \tag{4}$$

where the bundles B_i are seen as currents, ϕ_i are diffeomorphisms that deform the unknown template $\bar{B}$ supposed to be a current as well. ε_i are the residual perturbations which account for everything that cannot be captured by a regular deformation. The ε_i's are supposed to be i.i.d. zero-mean Gaussian random variables in the space of currents. To infer a random model on the deformations ϕ_i, we use their tangent-space representation: an instance ϕ^α is simulated by shooting geodesically an instance of the momenta α (vector of finite dimension).

We estimate the template $\bar{B}$, the deformations ϕ_i and the residues ε_i with a Maximum A Posteriori approach with an approximation, as in [4]. As a result, we minimize:

$$\min_{\bar{B}, \alpha_i} \left\{ \sum_{i=1}^N \left\| \phi^{\alpha_i} \star \bar{B} - B_i \right\|_{W^*}^2 + \gamma d_V^2(\mathrm{Id}, \phi^{\alpha_i}) \right\} \tag{5}$$

5

We start by setting $\phi_i = \text{Id}$ (i.e. $\alpha_i = 0$, no deformation) and $\bar{B} = \sum_{i=1}^{N} B_i/N$, the empirical mean in the space of currents. Then, we minimize the functional by considering that $\bar{B}$ and the α_i's are fixed alternatively. The first step consists in registering $\bar{B}$ to each B_i, leading to initial momenta (α_i). The second step consists in updating $\bar{B}$ by minimizing $J(\bar{B}) = \sum_{i=1}^{N} \left\| \phi^{\alpha_i} \star \bar{B} - B_i \right\|_{W^*}^2$. This last minimization benefits from the approximation scheme of [13, 4].

Eventually, the algorithm returns an unbiased template $\bar{B} = \sum_{k=1}^{n_B} \delta_{x_k}^{\tau_k}$ and the deformations ϕ^{α_i} of $\bar{B}$ to each B_i. We perform a PCA on the momenta (α_i), and another PCA on the residual perturbations $\varepsilon_i = \phi^{\alpha_i} \star \bar{B} - B_i$. We shoot geodesically in the direction (resp. in the opposite direction) of the first mode of momenta, m_α (resp. $-m_\alpha$), to give the first mode of deformation at $+\sigma$ (resp. $-\sigma$): $\phi^{\pm m_\alpha}$. The PCA on residues is performed in the space of currents. This leads to the mean $\bar{\varepsilon} = \sum_i \varepsilon_i/N$ and the first mode at $\pm\sigma$: $m_\varepsilon = \bar{\varepsilon} \pm \sum_i E_i(\varepsilon_i - \bar{\varepsilon})$, where E is the first eigenvector of the covariance matrix $(\langle \varepsilon_i - \bar{\varepsilon}, \varepsilon_j - \bar{\varepsilon} \rangle_{W^*})_{i,j}$. As linear combinations of the input currents, the mean and the first mode can be approximated using the scheme of [13] for a better visualization.

This joint statistical modeling accounts for both diffeomorphic and non-diffeomorphic variability. It is not biased by arbitrary point or fiber correspondences between different subjects. It does not impose strong prior on the nature of the variability. For instance, it does not assume that fibers of a bundle come from a mean line whose samples have been randomly moved, as in [9]. The major prior of our model consists in where to put the separation between the geometrical part (captured by the diffeomorphisms) and the texture part (contained in the residues). This separation is determined by the regularity parameters: λ_V, λ_W and the trade-off γ. In this paper, we set these parameters manually, whereas they could be set automatically along the lines of [16] for instance.

4 Experiments

Six brain DTI data sets acquired on a 1.5T GE scanner on healthy volunteers were used in this study. Image dimensions are $128 \times 128 \times 30$, and resolution is $1.8 \times 1.8 \times 4$mm. 25 non-collinear diffusion gradients and a b-value of $1000 s.mm^{-2}$ were used. Fiber tractography was performed using MedINRIA [5], which includes a robust tensor estimation and a streamline tractography algorithm using log-Euclidean tensor interpolation [17]. Manual segmentation of five fiber bundles was done: the entire corpus callosum, the corticospinal and the corticobulbar tracts, and the left and right arcuate fasciculi (Fig. 4-a).

First, we evaluate the methodology developed in Sec. 2 by registering the bundles of two subjects and comparing the result with FA and tensor registration (Sec. 4.1). Second, our framework for atlas construction is evaluated with the construction of a diffeomorphic atlas of the five bundles of our data set (Sec. 4.2) and the statistical analysis of the corticobulbar tract (Sec. 4.3).
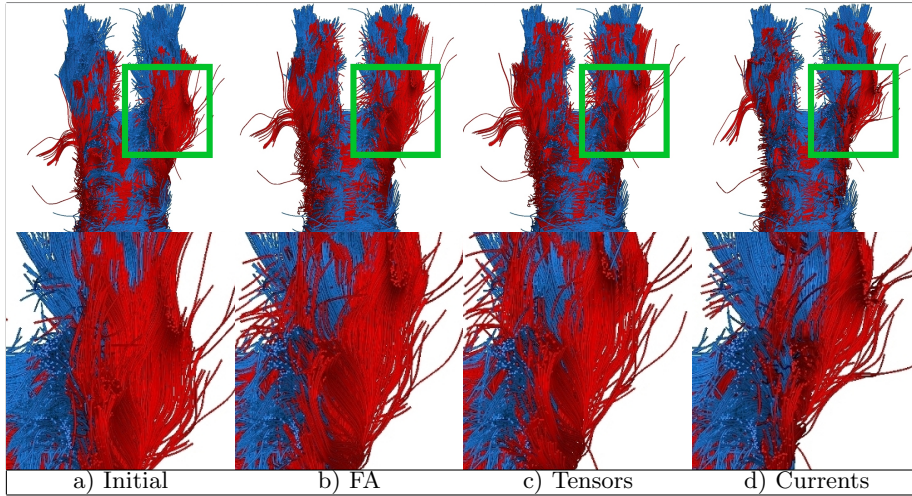
---

[5] http://www-sop.inria.fr/asclepios/software/MedINRIA/

Fig. 1. Diffeomorphic registration of two corpus callosum fibers. Bottom images are a closeup on the green squared region. Initial tracts (a) and registered tracts using FA (b), tensors (c) or bundles (d) as constraints. Overlap of blue and red fibers is greater using currents, especially in the left and right parts of the genu of the corpus callosum.

4.1 Fiber Bundle Registration

Diffeomorphic registration of fiber bundles using currents is compared to nonlinear registration of FA [18] and tensor [8] images. Pairwise registrations of 5 fiber bundles segmented in 2 subjects are conducted. For FA and tensor-based bundle registration, deformation fields were computed between images and applied to bundles afterwards: bundles were not tracked again after registration. Note that the three methods produce diffeomorphic transformations and can be compared. The parameters were adjusted to produce deformations of about the same smoothness. Concerning our registration scheme, we set the regularity of the deformation $\lambda_V = 20$mm, the spatial scale of the currents $\lambda_W = 5$mm and the trade-off between regularity and fidelity-to-data: $\gamma = 10^{-4}$. For clarity purpose, we present registration results of two bundles only: the corpus callosum (CC) (Fig. 1) and the corticospinal tract (CST) (Fig. 2), since they highlight the most striking differences between methods.

Fig. 1 a) shows two misaligned CC. Fig. 1 b) and c) present the registration of those bundles computed using respectively FA and tensor images. The registration of the fiber bundles with our method (Fig. 1 d) shows a greater overlap, synonym of a better alignment. Local improvements are noticeable in the left and right parts of the genu. This result shows that *the bundle information acts as a stronger prior* to align fiber tracts than the tensor image. Moreover, one can still notice few red fibers not aligned with the blue bundle in the exterior of the tract, which illustrates *the robustness of our methodology to outliers.*
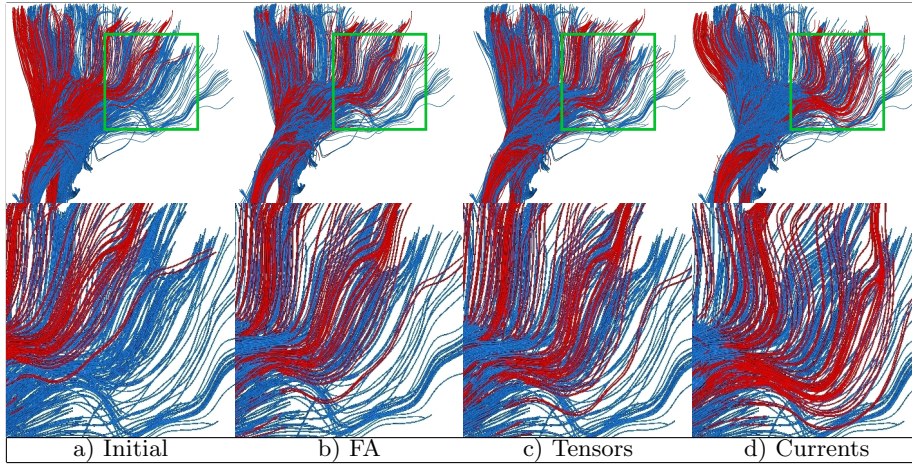
Fig. 2. Registration of two corticospinal tracts. Bottom images are a closeup on the green squared region. Initial tracts (a) and registered tract using FA (b), tensors (c) or bundles (d) as constraints. Currents better warp the red fibers in the anterior part of the tract, highlighting the aperture problem inherent to FA and tensor-based approaches. Registration in the posterior part is mainly constrained by the corpus callosum which strongly pushes the fibers toward the posterior part of the brain.
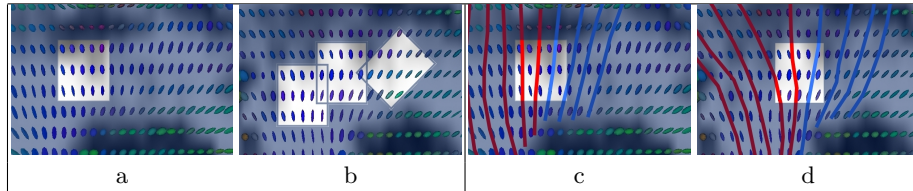

Fig. 3. Illustration of the aperture problem in FA and tensor registration. **a and b**: Tensor fields of two subjects overlapped with FA images are shown (sagittal slice, inside the corona radiata). Without any prior, it is impossible to determine whether the rectangle in image **a** matches with any in image **b**: this is the aperture problem. **c and d**: two schematic fiber bundles in red and blue were added. It becomes clearer that the rectangle of image **c** has a unique correspondence in image **d**. The aperture problem is partly solved using the bundles as priors.

Registration of two CST shows similar effects, especially in the anterior part expanded in a green square in Fig. 2. In those regions, multiple bundles may coexist whereas FA and tensor images are uniform, as shown in Fig. 3. Therefore, image-based registration is unable to correctly align the bundles, since bundle boundaries are not visible in images. This is an *aperture problem* inherent to FA and tensor-based methods. The bundling information is an extra information brought either by experts or by automatic bundling methods with anatomical priors. During our global registration, the CC acts as a stronger constraint than
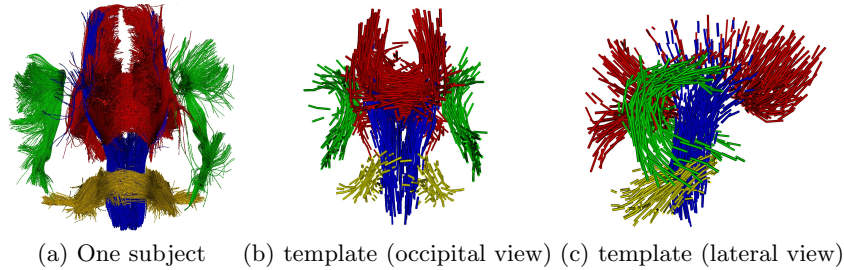
(a) One subject   (b) template (occipital view) (c) template (lateral view)

Fig. 4. Template of five bundles: the corticospinal tract (blue), the corticobulbar tract (yellow), the callosal fibers (red), the left and right arcuates (green). (a): one subject among the six of the data set. (b,c) the estimated unbiased atlas. Data result from a random deformation on the atlas, plus a random perturbation.

CST since it has much more fibers. This impacts the registration of the posterior part of the CST in Fig 2, whose fibers are pushed by the CC toward the posterior part of the brain. Although the method enables to adjust the weight of each bundle during registration, the choice of such weights still remain arbitrary.

4.2   Fiber Atlas Construction

As explained in Sec. 3, we estimate a template such that the input data result from random deformations of this template added with random perturbations in the space of currents. As emphasized in Section 2.2, there is only one global deformation acting on all 5 bundles together, and 5 independent perturbations for each bundle. The template consists of five prototype bundles shown in Fig. 4. It has been computed by fixing the parameters of currents $\lambda_W = 5$mm, of deformations $\lambda_V = 20$mm and the trade-off $\gamma = 10^{-4}$.

4.3   Variability Analysis of the Corticobulbar Tract

We show here how the first mode of deformations and the first mode of residues describe the variability of the corticobulbar tract within the studied population. The "geometrical" variability is captured by the deformations. As a result of the MAP estimation, the deformations appear to be centered: the norm of the mean parameters is 0.42 times the standard deviation, not significantly different from 0. The first mode of the deformations at $\pm\sigma$ is shown in Fig. 5, first row. It shows the variability of the template which was captured by the regular diffeomorphisms. The main variations are a torque of the frontal part of the bundle, as well as a stretching/shrinking of its lateral parts. Further investigation should determine whether this torque is related to the well-known brain torque.

The variability in terms of "texture" is captured by the residual perturbations. The residues are centered: the mean current is 0.36 times its standard deviation. The first residual mode m_ε is shown in Fig. 5, second row. It shows
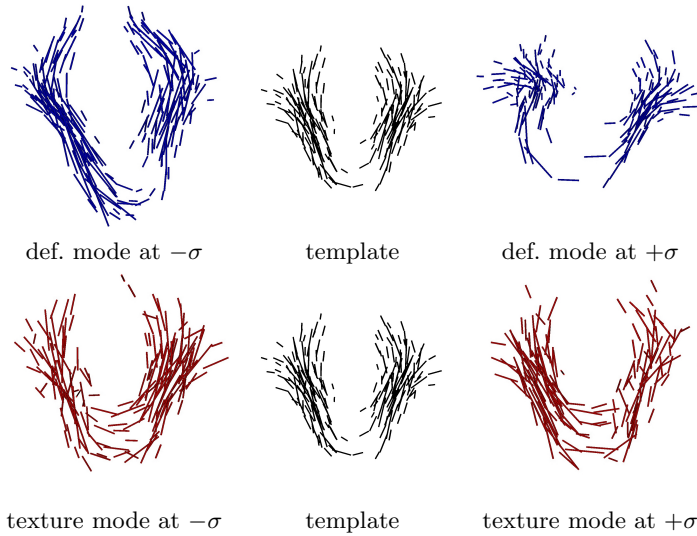
9

Fig. 5. Variability of the corticobulbar bundle (view from top) **Row 1: First deformation mode at** $\pm\sigma$. The diffeomorphic variability of the population around the prototype bundle (middle) is mainly a torque at the basis of the bundle and a stretching/shrinking effect of the left and right parts of the bundle. **Row 2: First "texture" mode at** $\pm\sigma$. The texture mode (what remains once the diffeomorphic variability is discounted) at $+\sigma$ (resp. $-\sigma$) shows that the left (resp. right) part of the bundle becomes thicker, while its right (resp. left) part becomes thinner.

an asymmetry in the number of fibers in each lateral part of the bundle. This result shows, undoubtedly, that the variability left aside from the diffeomorphisms is not pure noise, *but still contains some interesting anatomical features.* In our case, further investigation is needed to determine whether this fiber creation/deletion effect is due to a true anatomical variability or to an artifact of the tracking algorithm. In any case, this shows how our modeling analyzes all the geometrical information without imposing strong priors on the kind of the variations we are looking for.

5   Discussion and Conclusion

In this paper, we proposed a novel framework for the statistical analysis of fiber bundles using currents. Our methodology does not impose point-to-point or fiber-to-fiber correspondences, a crucial feature in regards to the variability of tractography algorithms outputs. It is also robust to outliers and weakly dependent of the fiber sampling. Diffeomorphic registrations produce smooth and invertible deformation fields which match consistently a set of fiber bundles of one subject onto another. This registration scheme is further extended by a

statistical model of fiber bundles, which estimates a template and its variability in a population. The variability is, in turn, decomposed into a geometrical part accounting for smooth deformations and a texture part which accounts for non-diffeomorphic changes in a population.

Pairwise registration shows that FA and tensor-based registration are less adapted than currents for fiber bundles registration, as bundle boundaries are not visible in those images (aperture problem). A misalignment of bundles may result in a loss of statistical power in group comparisons since contributions of several unrelated fiber bundles may be confounded. The method presented here optimally uses the strong prior that fibers belong to consistent bundles and ensure a proper alignment of those for statistical comparisons. This statistical analysis was evaluated on five fiber bundles extracted in six subjects. It shows consistent results with known anatomical variability (brain torque), which is put in evidence for the first time on fibers. Even with such a small dataset, our analysis managed to decompose the variability into two parts that are likely to describe relevant anatomical features.

The method, however, raises several questions. First, it is sensitive to the total number of fibers of a bundle, or fiber density, that may vary between two subjects. These variations may be caused by the tractography algorithm itself, as fiber density is generally an arbitrary parameter set by the method. One solution would consist in normalizing this density by relying the fiber density to physical properties of the neural fibers, like the neural flux transported by the bundle. Second, our method requires all fibers in a bundle, and by extension all bundles of different subjects, to have a consistent orientation: all fibers should start at the same cortical region and end in the same region. We cannot reasonably assume that tractography algorithms produce consistently oriented fibers. In this work, reorientation was performed with an empirical procedure. For larger datasets, an automatic reorientation procedure has to be included, or the modeling based on currents has to be adapted to account for non-oriented curves.

Future work will focus on evaluating the method on much larger dataset to strengthen the interpretation of our results. Automatic bundling can be used to produce a complete set of anatomically relevant fiber bundles, as in [19, 20]. Then, our measure of variability could be used to segment fiber bundles in new images. It could be used also to classify patients according to pathologies, to find consistent sub-groups within populations, to detect abnormalities via deviations from the normal variability. One can imagine to extend this framework to automatically mine geometrical dataset.

References

1. Durrleman, S., Pennec, X., Trouvé, A., Thompson, P., Ayache, N.: Inferring brain variability from diffeomorphic deformations of currents: an integrative approach. Medical Image Analysis **12**(5) (October 2008) 626–637

2. Fillard, P., Arsigny, V., Pennec, X., Hayashi, K., Thompson, P., Ayache, N.: Measuring brain variability by extrapolating sparse tensor fields measured on sulcal lines. NeuroImage **34**(2) (January 2007) 639–650

3. Vaillant, M., Miller, M., Younes, L., Trouvé, A.: Statistics on diffeomorphisms via tangent space representations. NeuroImage **23** (2004) 161–169

4. Durrleman, S., Pennec, X., Trouvé, A., Ayache, N.: A forward model to build unbiased atlases from curves and surfaces. In: Proc. of MFCA'08. (2008)

5. Goodlett, C., Fletcher, P., Gilmore, J., Gerig, G.: Group statistics of DTI fiber bundles using spatial functions of tensor measures. In: Proc. of MICCAI'08. Volume 3750 of LNCS. 1068–75

6. Smith, S., Jenkinson, M., Johansen-Berg, H., Rueckert, D., Nichols, T., Mackay, C., Watkins, K., Ciccarelli, O., Cader, M., Matthews, P., Behrens, T.: Tract-based spatial statistics: Voxelwise analysis of multi-subject diffusion data. NeuroImage **31** (July 2006) 1487–1505

7. Zhang, H., Yushkevich, P.A., Rueckert, D., , Gee, J.C.: Unbiased white matter atlas construction using diffusion tensor images. In: Proc. of MICCAI'07. Volume 4792 of LNCS. (2007) 211–218

8. Yeo, B., Vercauteren, T., Fillard, P., Pennec, X., Golland, P., Ayache, N., Clatz, O.: DTI registration with exact finite-strain differential. In: ISBI'08. (2008) 700–703

9. Corouge, I., Fletcher, P., Joshi, S., Gouttard, S., Gerig, G.: Fiber tract-oriented statistics for quantitative diffusion tensor MRI analysis. Medical Image Analysis (10) (2006) 786–798

10. Ziyan, U., Sabuncu, M.R., ODonnell, L.J., Westin, C.F.: Nonlinear registration of diffusion MR images based on fiber bundles. In: MICCAI'07. LNCS 4791 351–358

11. Batchelor, P.G., Calamante, F., Tournier, J.D., Atkinson, D., Hill, D.L.G., Connelly, A.: Quantification of the shape of fiber tracts. MRM **55**(4) (2006) 894–903

12. Vaillant, M., Glaunès, J.: Surface matching via currents. In: Proc. of IPMI'05. Volume 3565 of LNCS. (2005) 381–392

13. Durrleman, S., Pennec, X., Trouvé, A., Ayache, N.: Sparse approximation of currents for statistics on curves and surfaces. In: MICCAI'08. LNCS Vol. 5242 390–398

14. Saitoh, S.: Theory of Reproducing Kernels and Its Applications. Volume 189 of Pitman Research Notes in Mathematics Series. Wiley (1988)

15. Miller, M, I., Trouvé, A., Younes, L.: On the metrics and Euler-Lagrange equations of computational anatomy. Annual Review of Biomed. Eng. **4** (2002) 375–405

16. Allassonnière, S., Amit, Y., Trouvé, A.: Towards a coherent statistical framework for dense deformable template estimation. J. Roy. Stat. Soc. B **69**(1) (2007) 3–29

17. Fillard, P., Arsigny, V., Pennec, X., Ayache, N.: Clinical DT-MRI estimation, smoothing and fiber tracking with log-Euclidean metrics. IEEE Trans. on Medical Imaging **26**(11) (2007) 1472–1482

18. Vercauteren, T., Pennec, X., Malis, E., Perchant, A., Ayache, N.: Insight into efficient image registration techniques and the demons algorithm. In: Proc. of IPMI'07. Volume 4584 of LNCS. (2007) 495–506

19. Maddah, M., Wells, W.M., Warfield, S.K., Westin, C.F., Grimson, W.E.L.: Probabilistic clustering and quantitative analysis of white matter fiber tracts. In: Proc. of IPMI'07. Volume 4584 of LNCS. (2007) 372–383

20. El Kouby, V., Cointepas, Y., Poupon, C., Rivière, D., Golestani, N., Pallier, C., Poline, J.B., Bihan, D.L., Mangin, J.F.: MR diffusion-based inference of a fiber bundle model from a population of subjects. In: MICCAI'05. LNCS 3749 196–204